doi:10.1038/nature11097

Supplemental Text

Supplementary Figure 8 shows the zonal annual mean ensemble mean temperature trends for the CAM individual forcing experiments. Both black carbon (BC) and tropospheric ozone (TO3) yield maximum warming in the NH mid-latitudes, between 30-55N. Although this is in general agreement with the location of maximum increasing BC and TO3 trends (Supplementary Figures 1-2), differences do exist. Although we do not have a simple explanation, there is no real reason why warming should occur exactly where heat is added. Possible reasons for the mismatch likely involves latent heating effects, clouds, variations in radiative damping rates, or the land-ocean arrangement. In addition to the NH mid-latitude warming, both BC and TO3 yield NH high-latitude cooling. In terms of BC, this is consistent with reduced European emissions, resulting in negative zonal BC trends poleward of 55N. Both of these temperature responses contribute to a positive value of the Expansion Index (EI), since twice the mid-latitude warming exceeds the sum of low- and high-latitude warming. As Figure 4 shows, EI for BC is 0.15° decade^{-1} and 0.115° decade^{-1} for TO3. We expect a positive EI to be associated with poleward displacement of the tropospheric jet and the latitude of the maximum meridional temperature gradient (T_y). Supplementary Figures 9 and 10 show this to be the case. Both BC and TO3 feature reduced baroclinicity on the equatorward flank of the maximum (near 45N) and increased baroclinicity on the poleward flank. Similarly, both BC and TO3 feature reduced zonal winds (U) on the equatorward flank of the climatological jet and increased U on the poleward flank.

Supplementary Figure 11 shows that a geostrophic adjustment to the altered meridional temperature gradient explains most of the BC and TO3 response. Zonal wind shear for each pressure level is estimated from the corresponding meridional temperature gradient, according to thermal wind balance. To estimate the zonal wind, we use the 900 hPa zonal wind as a boundary condition. Taking a trend over the appropriate time period (1970-2009) yields the corresponding response, as shown in the center panel of Figure S11. The actual zonal wind trend closely corresponds to that estimated from thermal wind balance. The trend of the difference (estimate-actual) is generally small, although some significant differences do exist in the NH mid-latitudes. For example, the estimated trend shows a larger decrease in U on the equatorward flank of the jet.

Supplementary Figure 12 shows the tropospheric jet response, as well as the 500 hPa temperature response, occurs across all longitudes. The corresponding poleward tropospheric jet displacement is 0.11° decade^{-1} for both BC and TO3. We note a similar, but weaker response occurs for sulfate aerosols.

The Expansion Index also helps to explain why GHGs have resulted in less tropical expansion, compared to BC and TO3, over recent decades. Because GHGs are well-mixed throughout the atmosphere, they yield a more uniform warming of the troposphere, with the characteristic maxima in the tropical upper troposphere and at high-latitudes due to latent heating and snow/ice albedo effects, respectively. This results in a small, but positive value of the Expansion Index (0.06° decade^{-1}, about half as large as that for BC and TO3), which is consistent with the weaker poleward displacement of the maximum T_y and tropospheric jet (0.04° decade^{-1}).

To test the robustness of the CAM results, we conducted a series of simulations with the GFDL atmospheric model AM2.1 using climatological SSTs. Our first set of simulations investigated the equilibrium response to idealized mid-latitude heating. The experiment is forced with a mid-latitude (30-60°N/S) lower-tropospheric (surface to ~700 hPa) heating source of 0.4 K day^{-1}, and compared to a corresponding control simulation without the heat source. Both integrations were performed over 30 years, the last 20 of which are used to estimate the response. Supplementary Figure 13 shows the corresponding zonal annual mean temperature and zonal wind response. Maximum warming generally occurs at the heated latitudes, with some spillover to much of the troposphere. The weaker SH warming is likely due to the use of climatological SSTs, which leads to a heat sink over the Southern Ocean, and a smaller temperature increase. The zonal wind (U) response is consistent with a poleward jet displacement, as U increases on the poleward flank of the climatological jet, while decreasing on the equatorward flank, particularly in the NH where warming is largest. The corresponding poleward jet displacement is 1.98° in the NH and 0.45° in the SH, the former of which is significant at the 99% confidence level (based on a standard *t*-test using the pooled variance). Similar to the prior discussion, such a response is consistent with mid-latitude heating shifting the latitude of the maximum meridional temperature gradient (T_y)

poleward (now shown), and a corresponding geostrophic adjustment of the zonal winds, according to thermal wind balance.

Our second set of GFDL simulations investigated the tropospheric jet response to time-varying black carbon and tropospheric ozone, which have increased over much of the NH low- to mid-latitudes in recent decades. Similar to the CAM transient simulations, each of the ensemble members is integrated from an independent initial condition; the response is evaluated by comparing a simulation without BC or TO3 with a corresponding simulation with all time-varying forcings (GHGs, BC, OC, sulfate, ozone, solar and volcanic aerosols). A total of eight ensemble members were run. Unlike CAM, which used CMIP5 forcings, the GFDL time-varying forcing comes from GFDL's CMIP3 forcing data set. Aerosol concentrations, as well as tropospheric ozone, are obtained from the Model for Ozone and Related Chemical Tracers version 2.4 (MOZART-2) chemical transport model based on the EDGAR-HYDE emission inventory[44]. Emissions after year 2000 are based on the SRESA1B scenario. Both ozone and aerosol concentrations are therefore prescribed in GFDL AM2.1.

Supplementary Figure 14 shows the BC and TO3 annual mean ensemble mean temperature and zonal wind trend for 1979-2009. Similar to the CAM results, both BC and TO3 yield significant NH mid-latitude warming in the GFDL model, as well as a U response consistent with poleward displacement of the NH tropospheric jet—significant positive trends occur on the poleward flank of the climatological jet, while negative trends occur on the equatorward flank. The corresponding NH poleward jet displacement is also similar to that based on CAM at $0.11 \pm 0.18°$ decade^{-1} for BC and $0.16 \pm 0.19°$ decade^{-1} for TO3. We also note that the corresponding GFDL GHG response, like CAM, is less than half as large at $0.05 \pm 0.15°$ decade^{-1} (not shown). Thus, two different models with two different forcing inventories result in the same conclusion: BC and TO3, by preferentially warming the NH mid-latitudes, result in significant poleward jet displacement, which is larger than that associated with GHGs.

Supplemental References

44. Horowitz, L. W. Past, present, and future concentrations of tropospheric ozone and aerosols: Methodology, ozone evaluation, and sensitivity to aerosol wet removal. *J. Geophys. Res.* **111**, D22211 (2006)

doi:10.1038/nature11097

Supplementary Figures

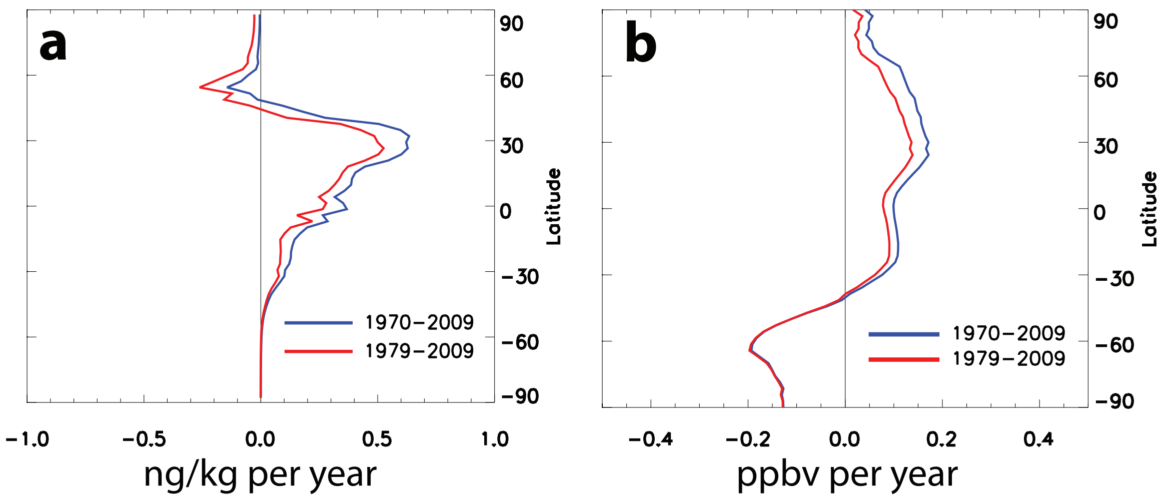

Figure S1. Zonal annual mean tropospheric trends for two time periods. (**a**) Black carbon; (**b)** Ozone. BC concentration trends include hydrophobic and hydrophilic BC and are based on CAM simulations using CMIP5 BC emissions. Ozone trends come directly from the CMIP5 forcing data set.

doi:10.1038/nature11097

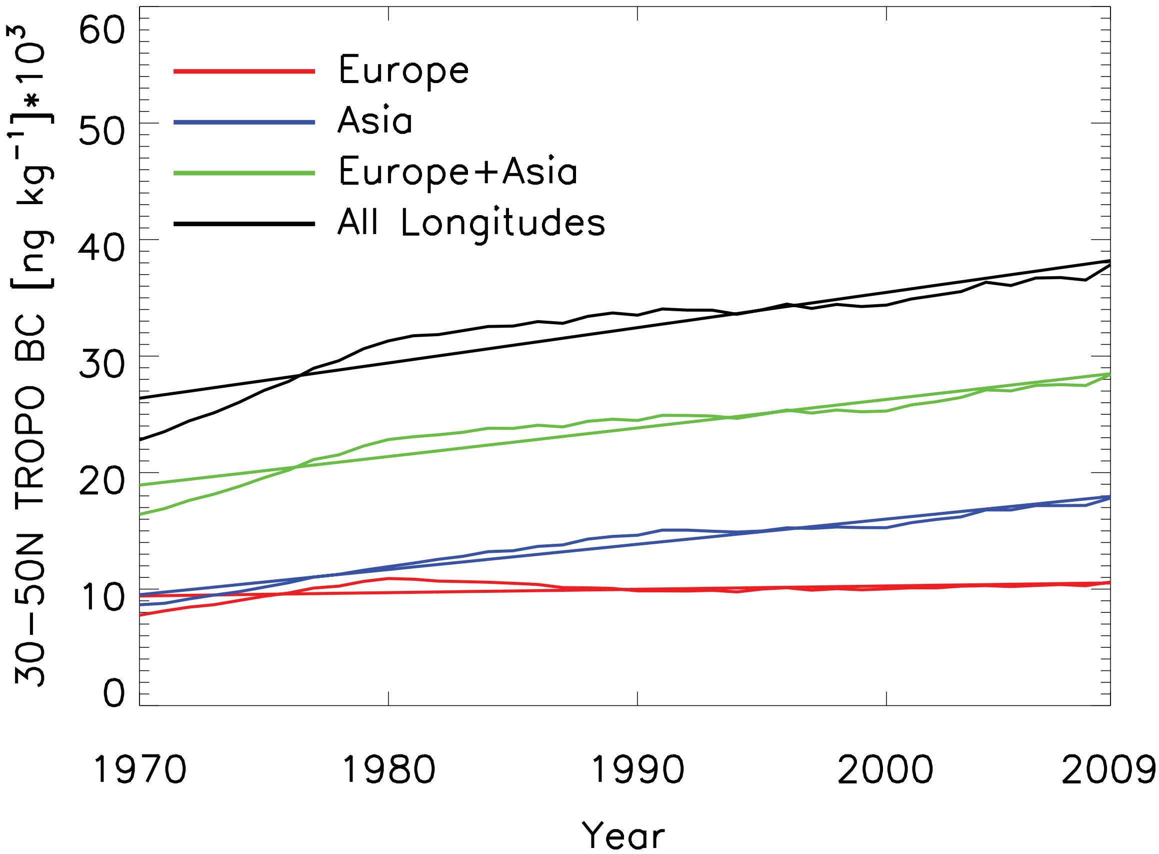

Figure S2. 1970-2009 annual mean time series and trend of tropospheric black carbon for select regions. Values are an area-weighted sum over "Europe" (30-50N; 0-90E), "Asia" (30-50N; 90-180E), both Europe and Asia (30-50N; 0-180E) and all longitudes (30-50N; 0-360E).

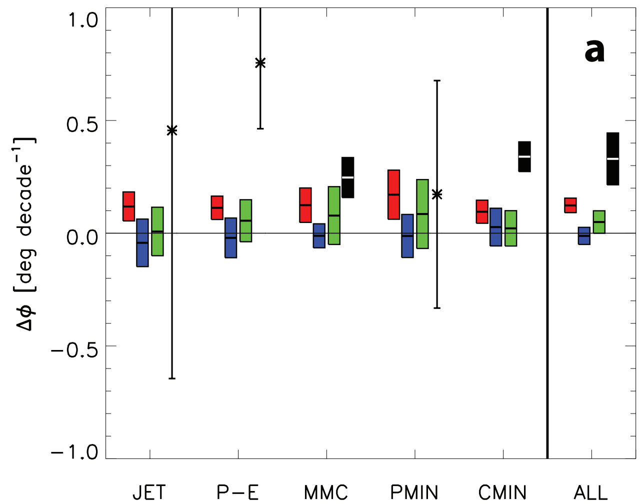

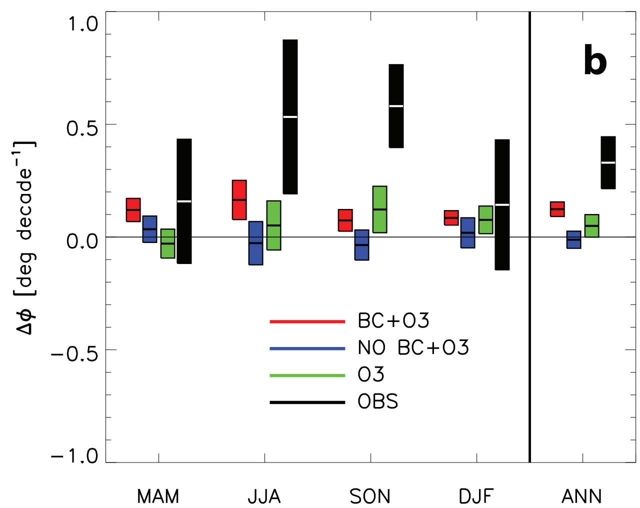

Figure S3. 1970-1999 CMIP3 Northern Hemisphere tropical expansion based on five metrics. (**a**) Annual mean poleward displacement of each metric, as well as the combined "ALL" metric. (**b**) Seasonal poleward displacement of all metrics combined. CMIP3 models are grouped by the 9 models that included time-varying BC and ozone (red); the 3 models that included time-varying ozone only (green); and the 6 models that did not include time varying BC or ozone (blue). Boxes show the mean response (center line) and its 2-sigma uncertainty. In the case of one observational data set (i.e., JET, P-E and PMIN), uncertainty is estimated as the 95% confidence level, accounting for autocorrelation. Also included are observations based on 1979-1999.

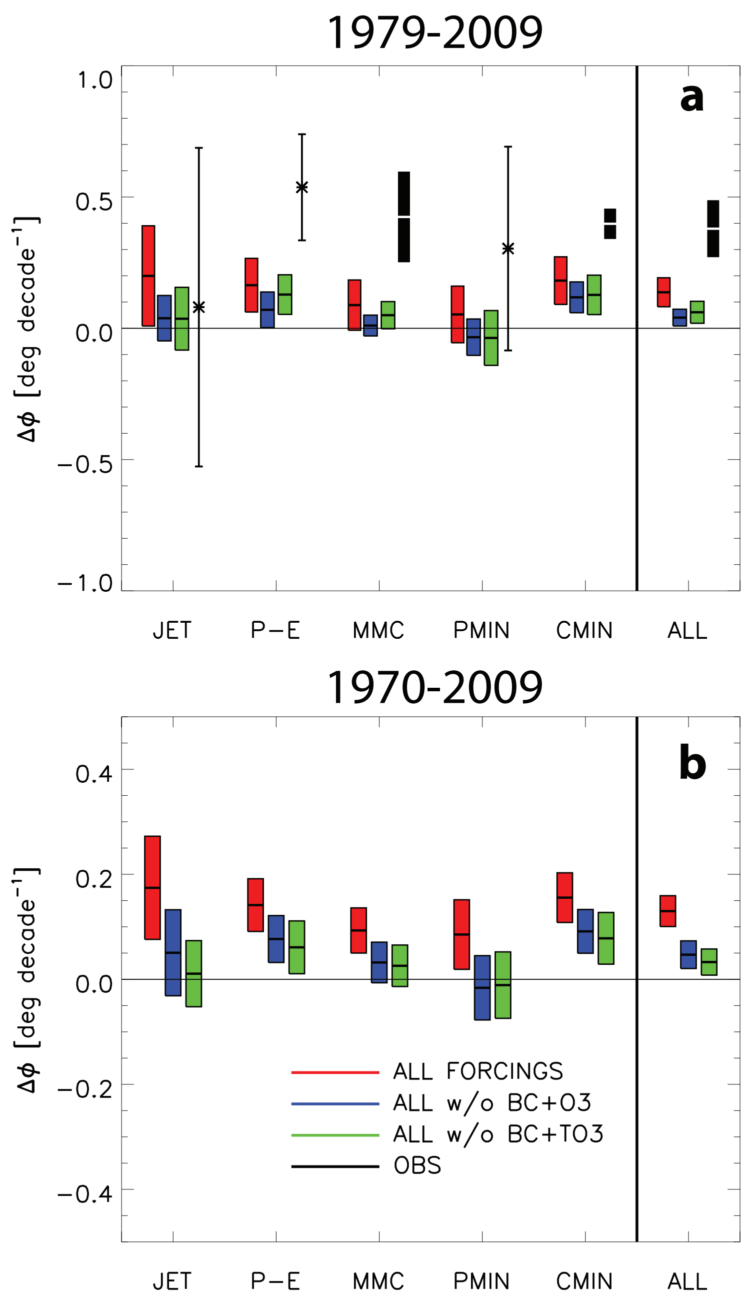

Figure S4. Northern Hemisphere annual mean tropical expansion based on five metrics for CAM3 experiments. (**a**) 1979-2009; (**b**) 1970-2009. Observations are also included for the 1979-2009 time period. Boxes show the mean response (center line) and its 2-sigma uncertainty. In the case of one observational data set (i.e., JET, P-E and PMIN), uncertainty is estimated as the 95% confidence level, accounting for autocorrelation.

doi:10.1038/nature11097

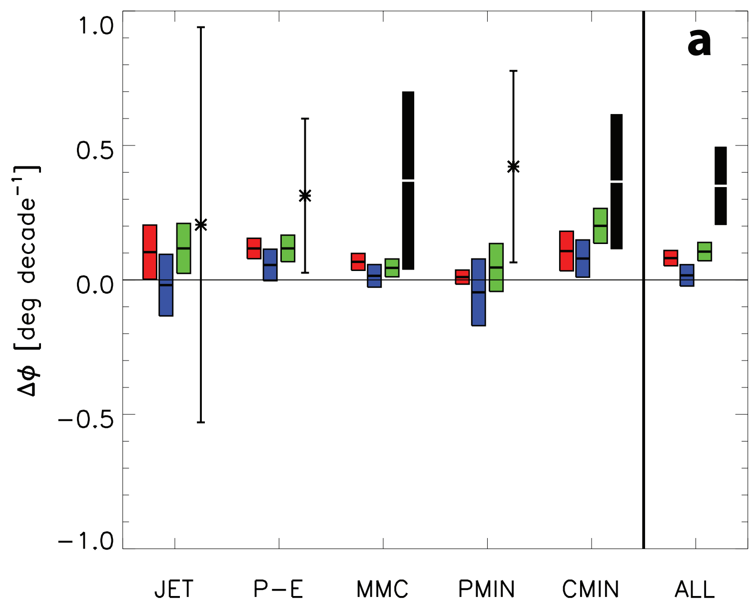

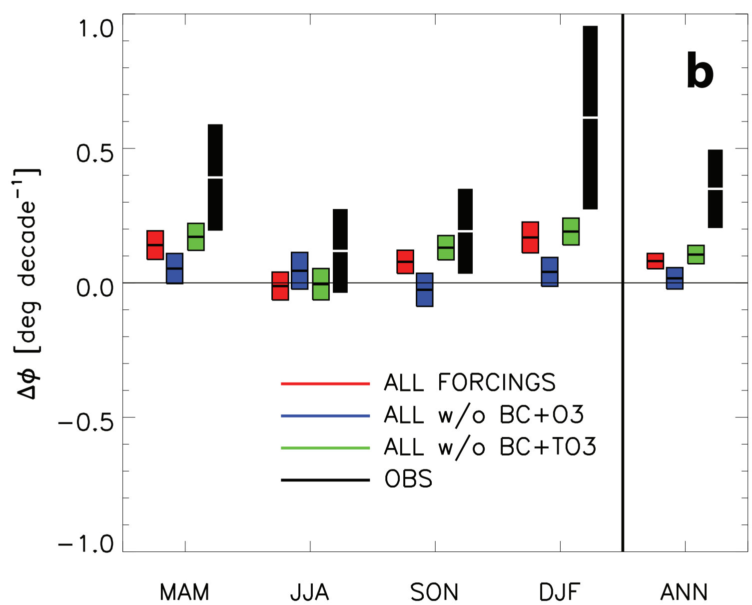

Figure S5. 1979-2009 Southern Hemisphere tropical expansion based on CAM3 experiments and observations. (**a**) Annual mean poleward displacement for each metric separately, and the combined metric. (**b**) Seasonal displacement of the combined "ALL" metric. Boxes show the mean response (center line) and its 2-sigma uncertainty. In the case of one observational data set (i.e., JET, P-E and PMIN), uncertainty is estimated as the 95% confidence level, accounting for autocorrelation.

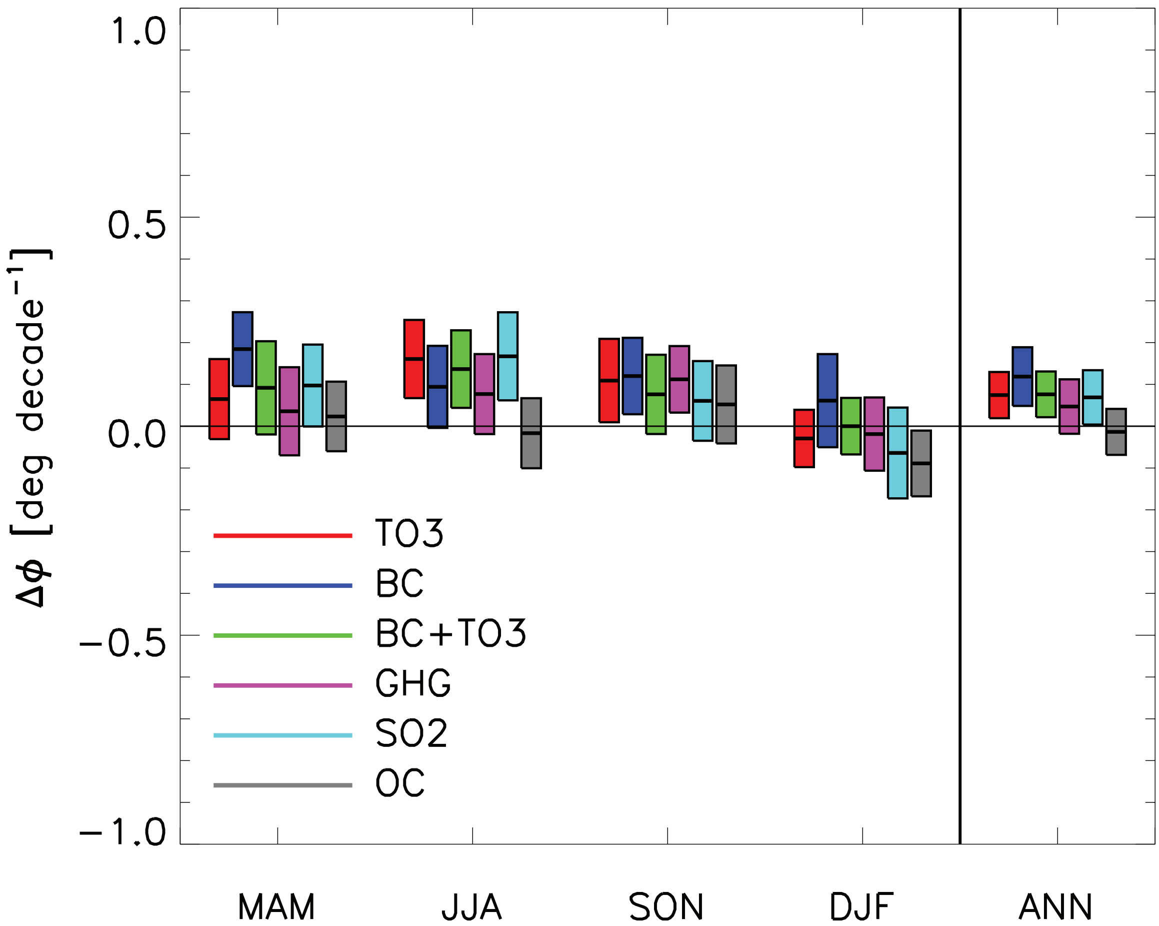

Figure S6. 1979-2009 Northern Hemisphere seasonal tropical expansion for individual forcings. Panels show the difference between CAM experiments with all forcings and all forcings without (red) tropospheric ozone, (blue) black carbon, (green) black carbon and tropospheric ozone, (purple) GHGs, (light blue) sulfate, and (gray) organic carbon. Boxes show the mean response (center line) and its 2-sigma uncertainty.

doi:10.1038/nature11097

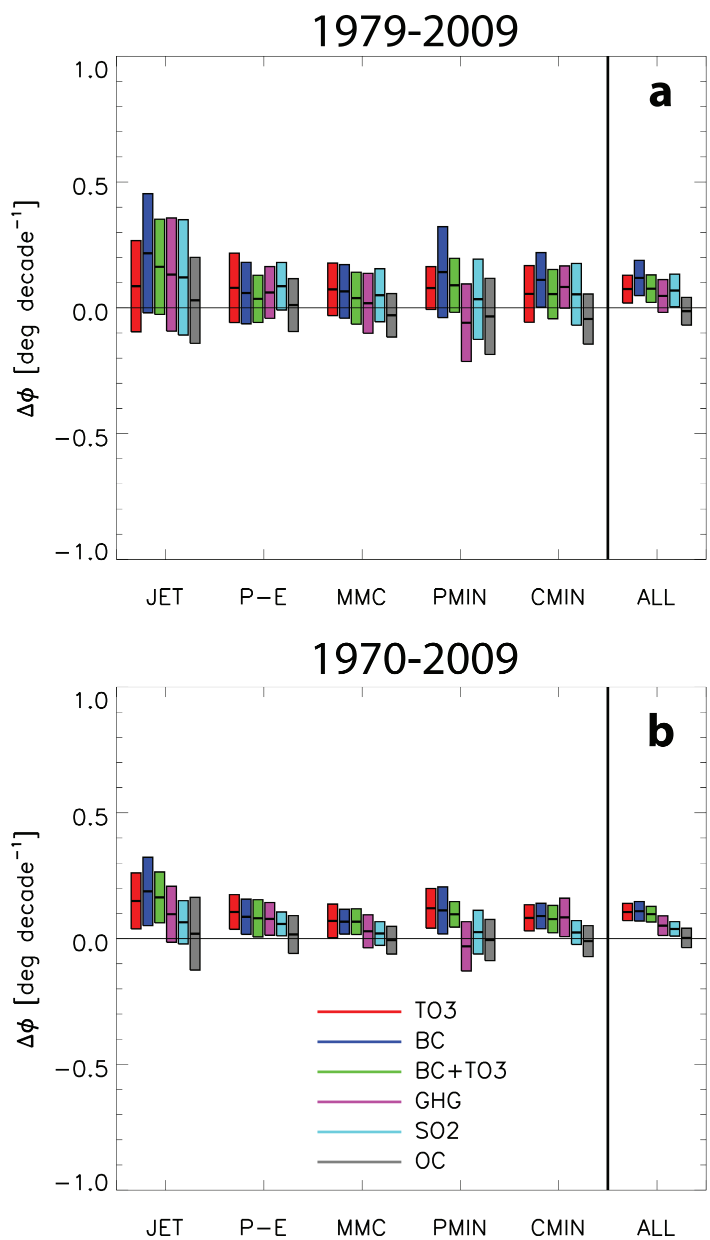

Figure S7. Northern Hemisphere annual mean tropical expansion based on five metrics, and the combined "ALL" metric. (**a**) 1970-2009; (**b**) 1970-2009. Panels show the difference between CAM experiments with all forcings and all forcings without (red) tropospheric ozone, (blue) black carbon, (green) black carbon and tropospheric ozone, (purple) GHGs, (light blue) sulfate, and (gray) organic carbon. Boxes show the mean response (center line) and its 2-sigma uncertainty.

doi:10.1038/nature11097

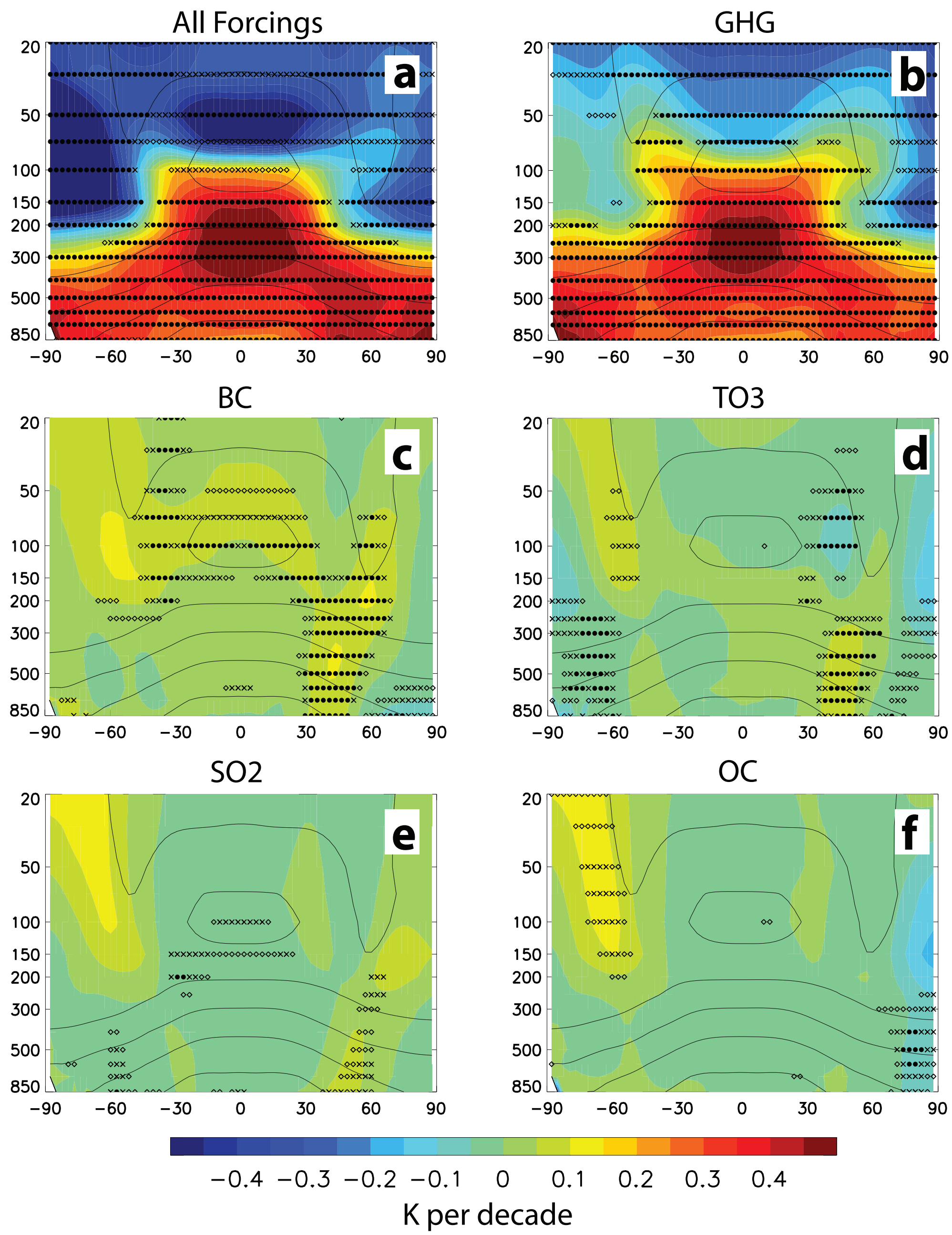

Figure S8. 1970-2009 zonal annual mean ensemble mean temperature trends for the listed CAM experiments. Except for the all forcings experiment, trends are estimated from the difference series of the all forcing experiment, and the corresponding all forcing experiment without a given forcing agent. Thin black lines show the climatological temperature [K]. Symbols represent significance at the 90% (diamond); 95% (cross) and 99% (dot) confidence level, accounting for autocorrelation.

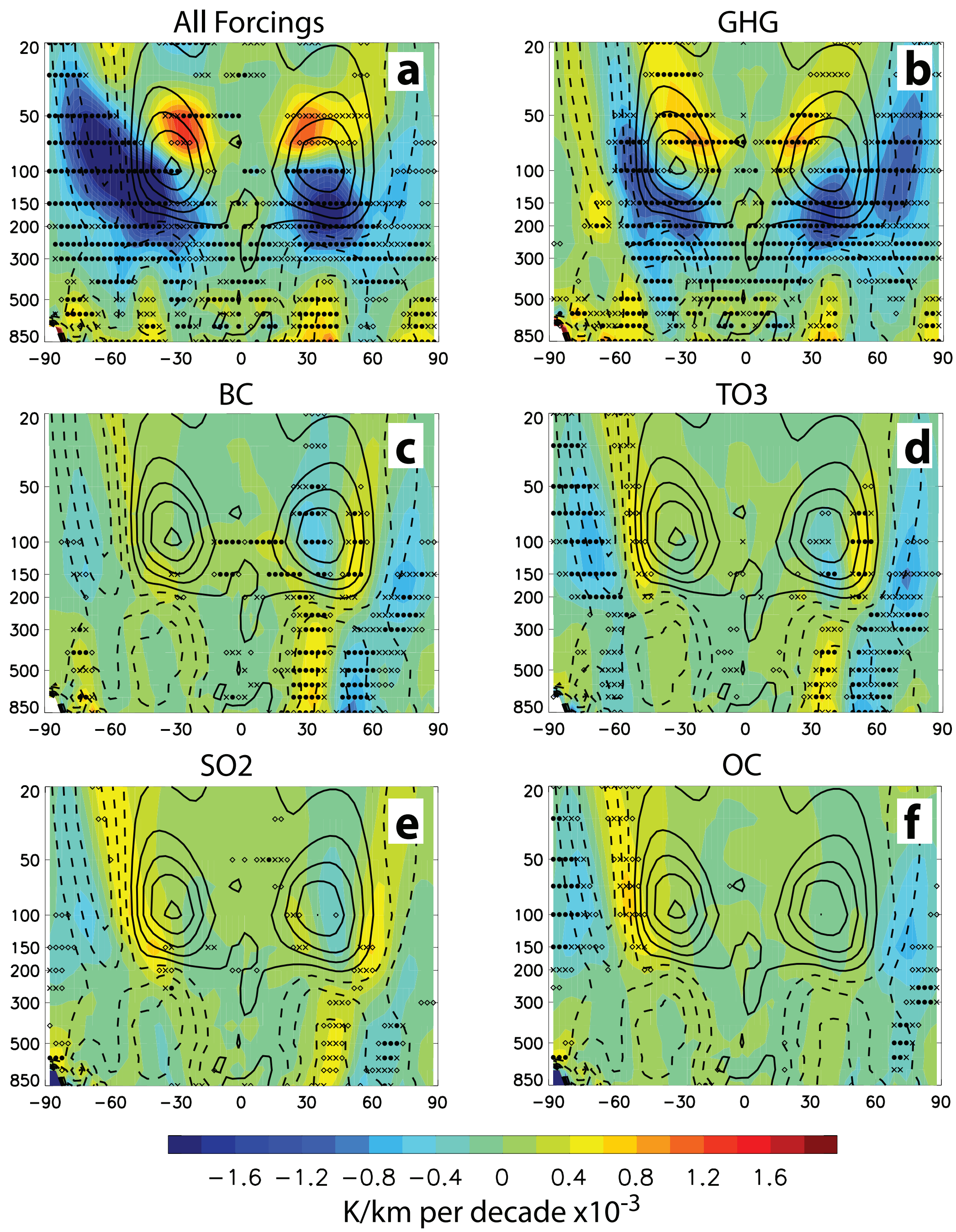

Figure S9. 1970-2009 zonal annual mean ensemble mean temperature gradient trends for the listed CAM experiments. Thin black lines show the climatological zonal temperature gradient [K km^{-1}x10^{-3}]. Southern hemisphere values have been multiplied by -1 such that negative contours always represent colder air polewards. Symbols represent significance as in Fig. S8.

doi:10.1038/nature11097

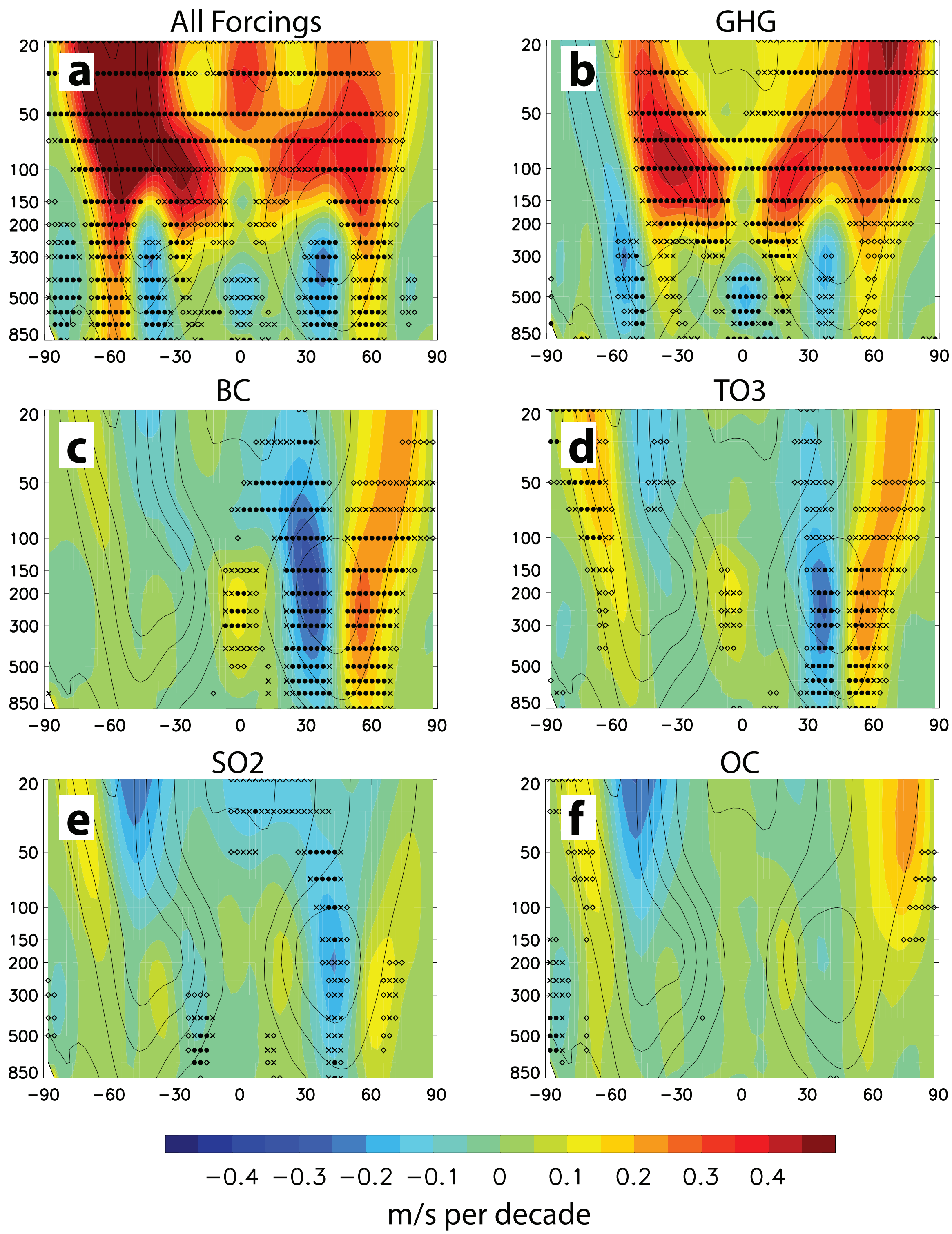

Figure S10. 1970-2009 zonal annual mean ensemble mean zonal wind trends for the listed CAM experiments. Thin black lines show the climatological zonal winds [m s^{-1}]. Symbols represent significance as in Fig. S8.

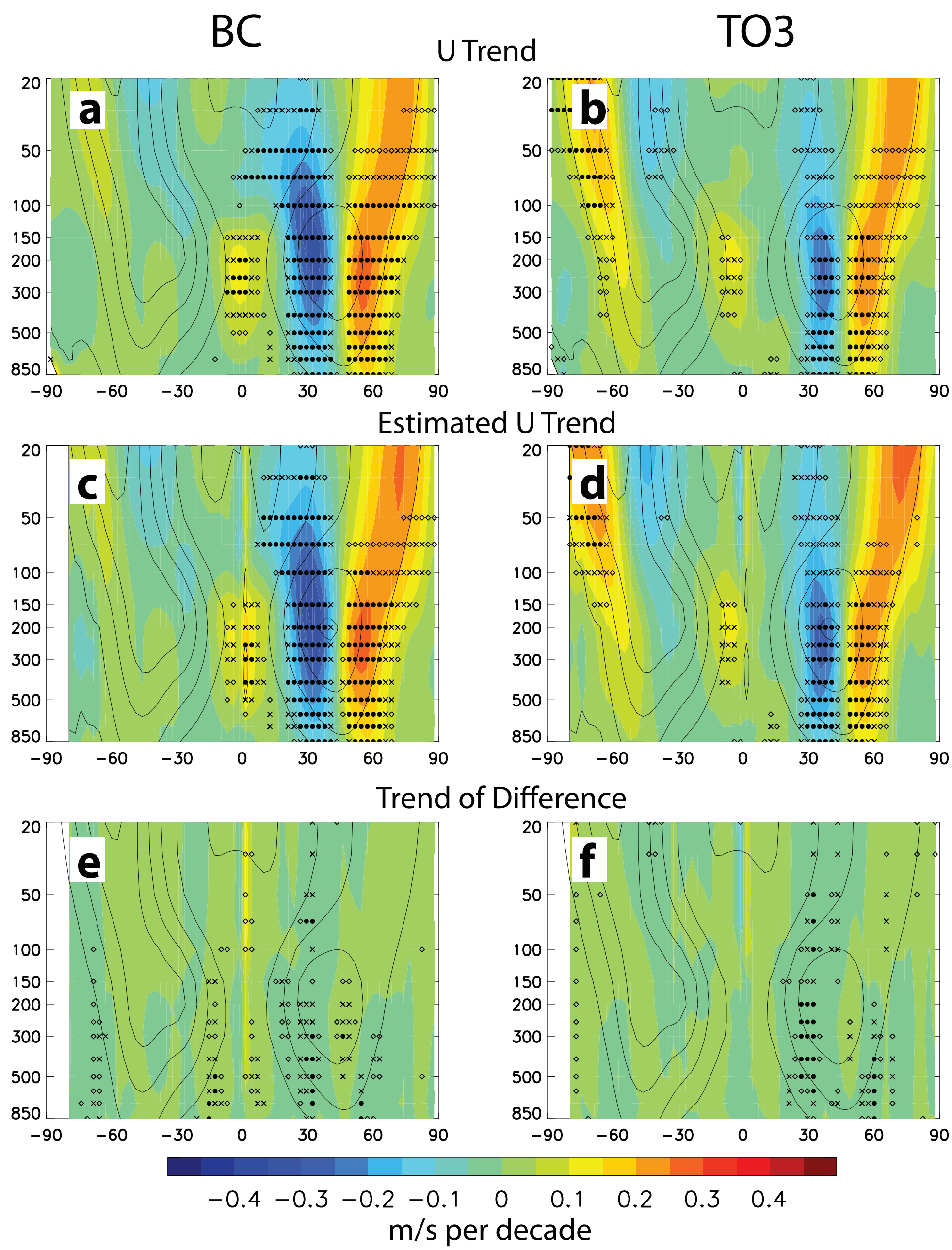

Figure S11. 1970-2009 zonal annual mean ensemble mean zonal wind trends for the CAM BC and TO3 experiments. **(a,b)** Actual U trend (as in Fig. S10); **(c,d)** Estimated U trend; **(e,f)** Trend of difference (estimate-actual). The estimated U trend is based on thermal wind balance, using the 900 hPa winds as a lower boundary condition. Thin black lines show the climatological zonal winds [m s^{-1}]. Symbols represent significance as in Fig. S8.

doi:10.1038/nature11097

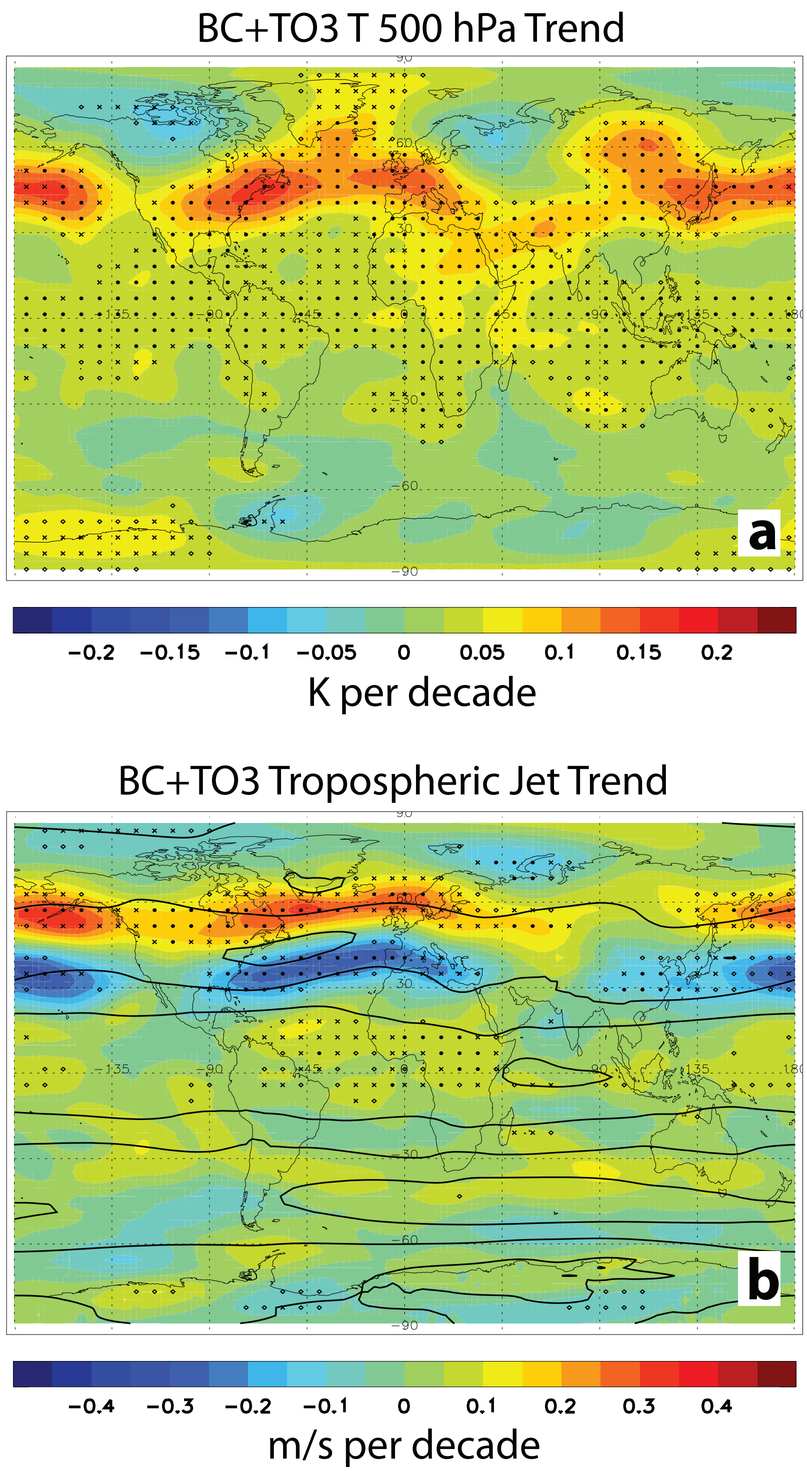

Figure S12. 1970-2009 annual mean ensemble mean 500 hPa spatial trends for the BC+TO3 CAM experiment. (**a**) temperature; (**b**) Tropospheric zonal wind. Thin black lines show the climatological jet [m s^{-1}]. Symbols represent significance as in Fig. S8.

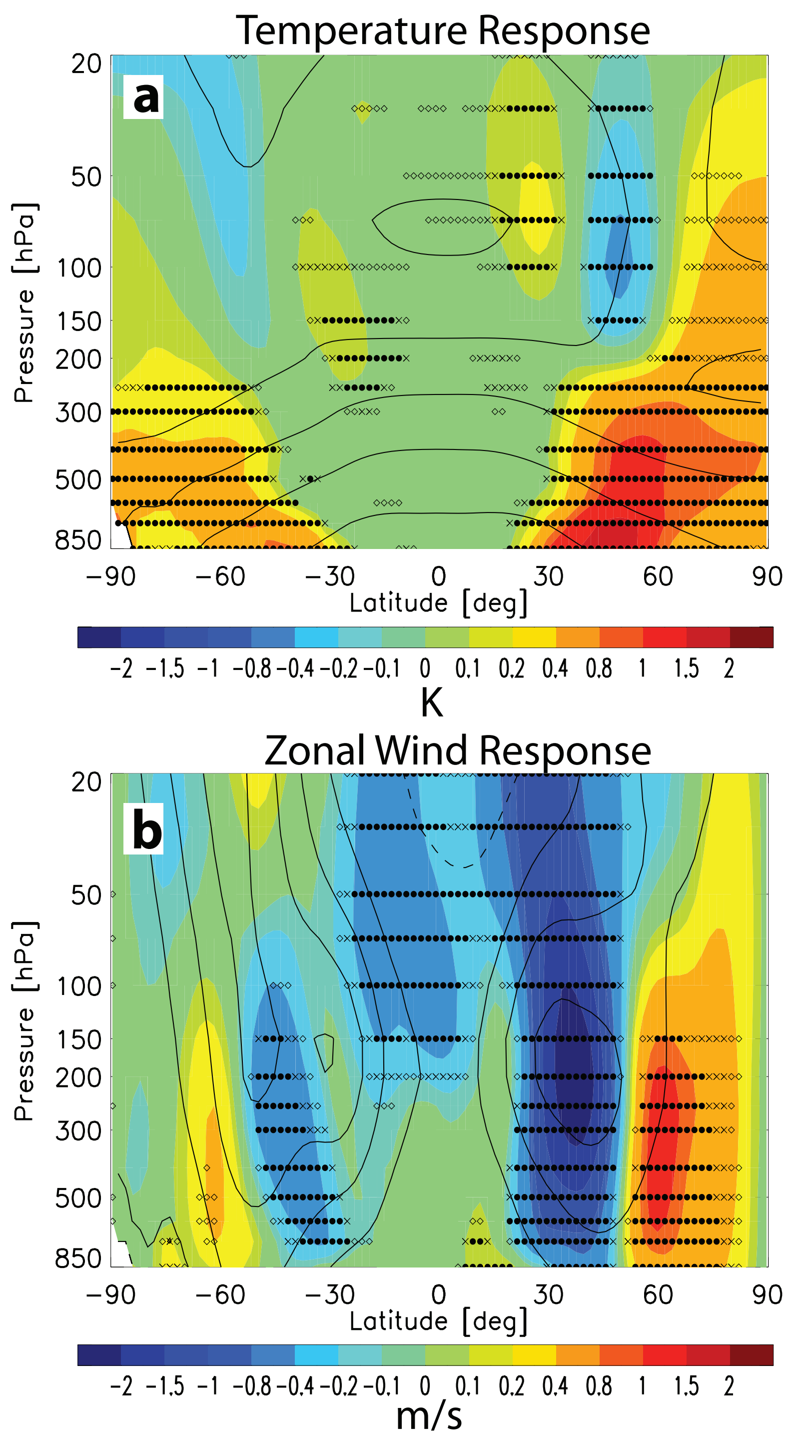

Figure S13. Zonal annual mean temperature and zonal wind response for GFDL AM2.1 equilibrium experiments for idealized mid-latitude heating. Thin black lines show the climatological values. Symbols represent significance as in Fig. S8.

doi:10.1038/nature11097

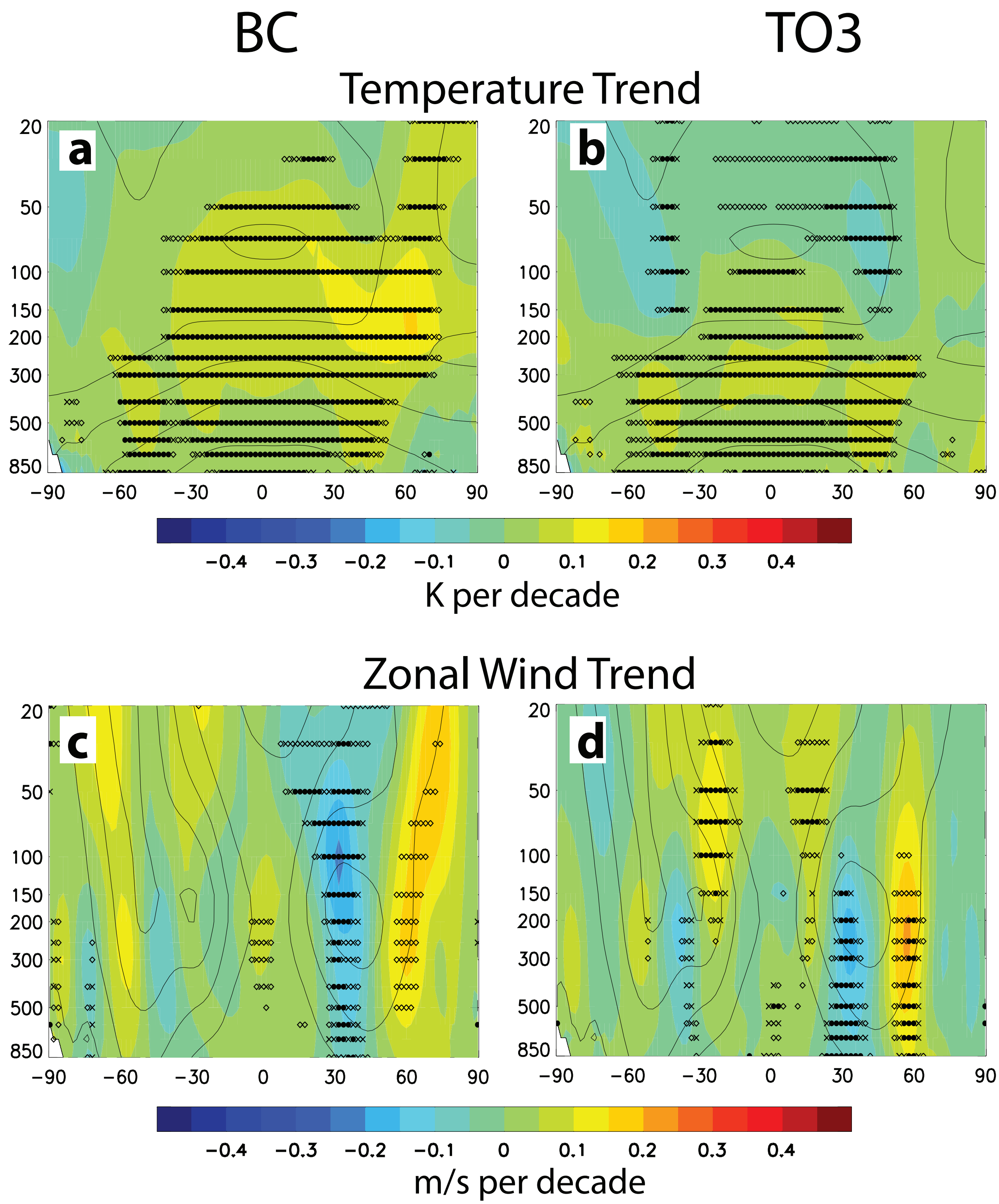

Figure S14. 1979-2009 zonal annual mean ensemble mean temperature and zonal wind trends for GFDL AM2.1 transient experiments. (**a,c**) Black carbon; (**b,d**) Tropospheric ozone. Symbols represent significance as in Fig. S8.

doi:10.1038/nature11097

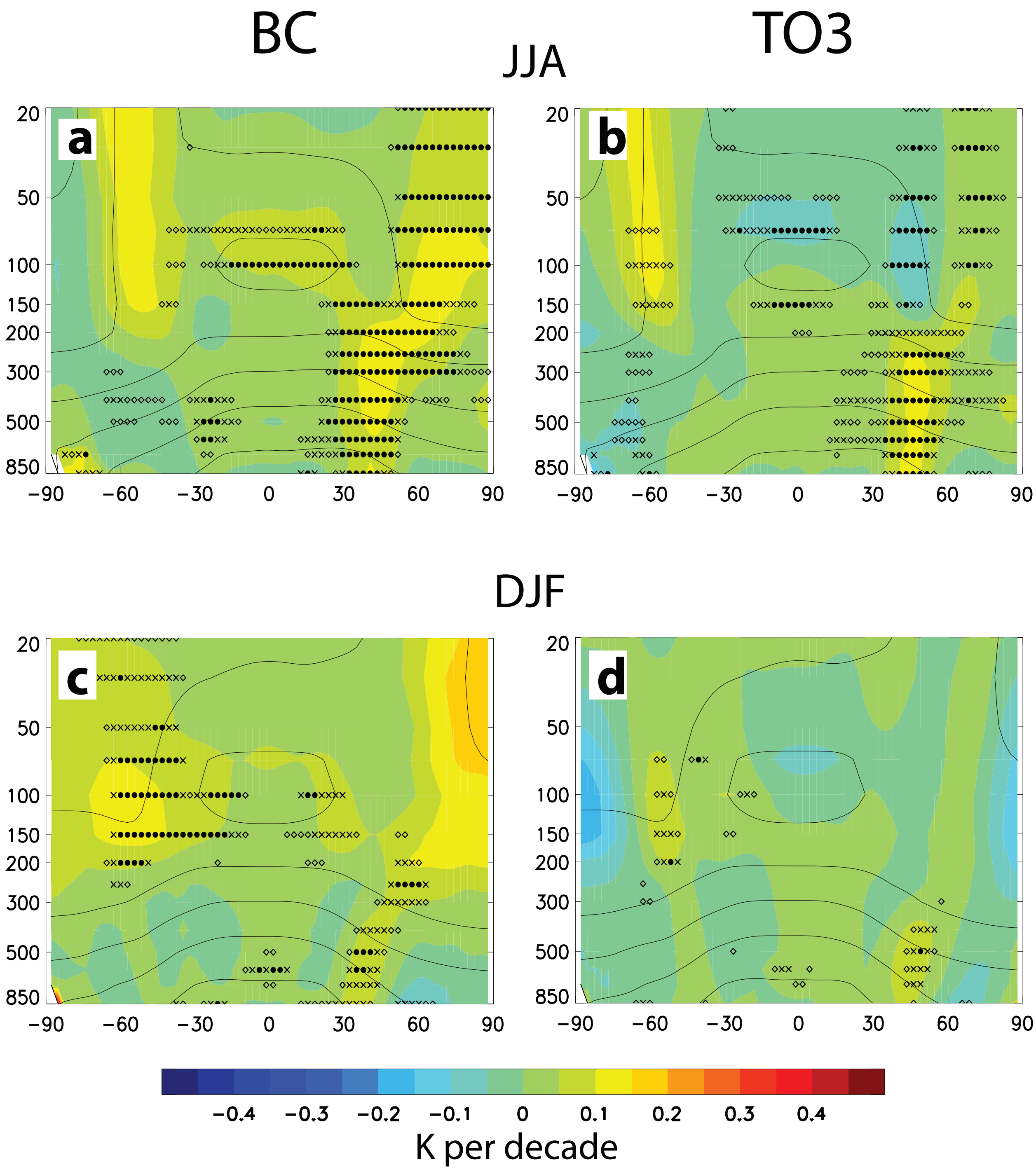

Figure S15. 1970-2009 zonal mean ensemble mean seasonal temperature trends for CAM BC and TO3 experiments. (**a**,**b**) June-July-August; (**c**,**d**) December-January-February. Thin black lines show the climatological temperature [K]. Symbols represent significance as in Fig. S8.

doi:10.1038/nature11097

Supplementary Tables

Model Acronym	Institution	ES
CCSM3	National Center for Atmospheric Research	8
CNRM-CM3	Meteo-France/CNRM	1
GFDL-CM2.0	Geophysical Fluid Dynamics Laboratory	3
GFDL-CM2.1	Geophysical Fluid Dynamics Laboratory	3
GISS-EH	Goddard Institute for Space Studies	5
GISS-ER	Goddard Institute for Space Studies	9
MIROC3.2 (medres)	Center for Climate System Research/NIES/JAMSTEC	3
MIROC3.2 (hires)	Center for Climate System Research/NIES/JAMSTEC	1
UKMO-HadGEM1	Hadley Center for Climate Prediction and Research	2
PCM	National Center for Atmospheric Research	4
UKMO-HadCM3	Hadley Centre for Climate Prediction and Research	2
ECHAM5/MPI-OM	Max-Planck Institute for Meteorology	3
CCCma-CGCM3.1(T47)	Canadian Center for Climate Modeling and Analysis	5
CCCma-CGCM3.1(T63)	Canadian Center for Climate Modeling and Analysis	3
FGOALS-g1.0	Institute for Atmospheric Physics	3
INM-CM3.0	Institute for Numerical Mathematics	1
IPSL-CM4	Institute Pierre Simon Laplace	1
MRI-CGCM2.3.2	Meteorological Research Institute	1

Table S1. Definition of the 18 CMIP3 models. ES is the number of independent realizations of the 20th century climate change experiment. The first 9 models include time-varying black carbon (BC) and ozone forcing, with changes on interannual and longer time scales; the next 3 models including time-varying ozone forcing but lacked time-varying BC; and the last 6 models lacked time-varying BC and ozone.